Published in final edited form as:
Cancer Res. 2008 May 15; 68(10): 3697–3706. doi:10.1158/0008-5472.CAN-07-6702.

The Nuclear Receptor Coactivator Amplified in Breast Cancer-1 Is Required for *Neu* (ErbB2/HER2) Activation, Signaling, and Mammary Tumorigenesis in Mice

Mark P. Fereshteh[1,2], **Maddalena T. Tilli**[1], **Sung Eun Kim**[1], **Jianming Xu**[3], **Bert W. O'Malley**[3], **Anton Wellstein**[1,2], **Priscilla A. Furth**[1], and **Anna T. Riegel**[1,2]

[1]Department of Oncology, Lombardi Comprehensive Cancer Center, Georgetown University, Washington, District of Columbia

[2]Department of Pharmacology, Lombardi Comprehensive Cancer Center, Georgetown University, Washington, District of Columbia

[3]Department of Molecular and Cellular Biology, Baylor College of Medicine, Houston, Texas

Abstract

Overexpression of the oncogene amplified in breast cancer 1 (AIB1)/steroid receptor coactivator-3 (SRC-3) induces mammary tumorigenesis in mice. In breast cancer, high levels of AIB1/SRC-3 and the growth factor receptor HER2/*neu* predict resistance to endocrine therapy and poor outcome. However, a mechanistic relationship between AIB1/SRC-3 and HER2/*neu* in the development of breast cancer has not been shown. Here, we show that deletion of one allele of *SRC-3* significantly delays *Neu*-induced mammary tumor development in mice. Homozygous deletion of SRC-3 in mice completely prevents *Neu*-induced tumor formation. By ages 3 to 4 months, *Neu*/SRC-$3^{+/-}$ mice exhibit a noticeable reduction in lateral side-bud formation, accompanied by reduced cellular levels of phosphorylated *Neu* compared with *Neu*/SRC-3^{wt} mice. In *Neu*-induced tumors, high levels of SRC-3, phosphorylated *Neu*, cyclin D1, cyclin E, and proliferating cell nuclear antigen expression are observed, accompanied by activation of the AKT and c-Jun NH_2 kinase (JNK) signaling pathways. In comparison, phosphorylated *Neu*, cyclin D1, and cyclin E are significantly decreased in *Neu*/SRC-$3^{+/-}$ tumors, proliferation is reduced, and AKT and JNK activation is barely detectable. Our data indicate that AIB1/SRC-3 is required for HER2/*neu* oncogenic activity and for the phosphorylation and activation of the HER2/*neu* receptor. We predict that reducing AIB1/SRC-3 levels or activity in the mammary epithelium could potentiate therapies aimed at inhibiting HER2/*neu* signaling in breast cancer. [Cancer Res 2008;68(10):3697–706]

Introduction

The nuclear receptor coactivator 3 [amplified in breast cancer 1 (AIB1)/steroid receptor coactivator-3 (SRC-3)] is the only steroid receptor coactivator family member that is amplified and overexpressed in several types of human epithelial tumors, such as breast and

Requests for reprints: Anna T. Riegel, Department of Oncology, Lombardi Comprehensive Cancer Center Research Building, Georgetown University, 3970 Reservoir Road, NRB E311, Washington, DC 20057. Phone: 202-687-1479; Fax: 202-687-4821; ariege01@georgetown.edu.

Supplementary data for this article are available at Cancer Research Online (http://cancerres.aacrjournals.org/).

Disclosure of Potential Conflicts of Interest
No potential conflicts of interest were disclosed.

prostate cancer (1–3). The *AIB1/SRC-3* gene is amplified on chromosome 20q in 5% to 10% of human breast cancers and is overexpressed at both mRNA and protein levels in ~30% of breast cancer cell lines and breast tumors (1, 2, 4). The overexpression of AIB1/SRC-3 or AIB1-Δ3 (a potent isoform of AIB1; ref. 5) in transgenic mice increased mammary epithelial cell proliferation, insulin-like growth factor I (IGF-I) signaling and initiated the development of mammary hyperplasia and tumorigenesis (6, 7). SRC-3 knockout (SRC-$3^{-/-}$) mice display decreased mammary gland development during pregnancy, abnormal reproductive function, and mammary gland growth retardation (8, 9). The loss of SRC-3 in mouse mammary tumor virus (MMTV)/v-Haras mice suppresses mammary gland ductal hyperplasia, mammary gland tumorigenesis, and IGF-I signaling (8–10). We have shown that loss of AIB1/SRC-3 in MCF-7 breast cancer cells decreases IGF-I signaling, IGF-I receptor expression levels, and IGF-I–induced anchorage-independent growth (11). Consistent with a central role for AIB1/SRC-3 in growth factor signaling, we recently reported that AIB1/SRC-3 knockdown by small interfering RNA (siRNA) decreases epidermal growth factor [EGF; EGF receptor (EGFR)/HER1] phosphorylation and EGFR-dependent downstream mitogenic signaling (12). Taken together, the observations in animal and *in vitro* models indicate that AIB1/SRC-3 plays a significant role in several growth factor–induced pathways that are relevant to breast cancer cell survival and proliferation.

One of the most important oncogenes in human breast cancer is the HER2/*neu* growth factor receptor tyrosine kinase, which belongs to the EGFR/HER family. HER2/*neu*–positive breast cancer responds to the monoclonal antibody trastuzumab; however, patients frequently develop resistance to the therapy. HER2/*neu* is amplified and overexpressed in 30% of human breast cancers, and its expression is correlated with negative prognosis and shortened disease-free survival (13). It has been reported that the overexpression of HER2/*neu* is correlated with high AIB1/SRC-3 mRNA levels in primary breast tumors (14). The overexpression of AIB1/SRC-3 was also found to be correlated with increased HER2/*neu* expression and resistance to tamoxifen in ER-positive breast cancer patients (15–17). These findings suggest that the biological roles of AIB1/SRC-3 and HER2/*neu* are linked in breast cancer and that AIB1/SRC-3 may increase the sensitivity of breast cancer cells to HER2/*neu*–driven tumorigenesis.

To assess the importance of the interplay between AIB1/SRC-3 and *Neu* in the development and progression of mammary cancer, we generated MMTV-*Neu*/SRC-$3^{+/-}$ and MMTV-*Neu*/SRC-$3^{-/-}$ mice. The MMTV-*Neu* mouse model overexpresses wild-type *Neu* in the mammary glands, resulting in an activating transmembrane mutation in the *Neu* transgene that promotes mammary tumorigenesis (18, 19). This model is ideal for studying the role of AIB1/SRC-3 in *Neu*-driven mammary tumorigenesis because it closely mimics the progression of human breast epithelial neoplasia, driven by the amplification and overexpression of the human homologue of HER2/*neu* (ErbB2; ref. 13). Our studies revealed that MMTV-*Neu* mice, with reduced SRC-3 levels, show a reduction in *Neu* phosphorylation. This led to a significant decrease in *Neu*-dependent downstream signaling and cell proliferation during the progression of mammary tumorigenesis. These data provide evidence that AIB1/SRC-3 plays a major role in the oncogenic activity of HER2/*neu* in the breast, thus making it an attractive therapeutic target in mammary tumors expressing HER2/*neu*.

Materials and Methods

Mice

The MMTV-*Neu* transgenic line was purchased from the Jackson Laboratory and previously described (19). *Neu*/SRC-3^{wt}, *Neu*/SRC-$3^{+/-}$, and *Neu*/SRC-$3^{-/-}$ mice were generated by

crossing the SRC-$3^{+/-}$ mice with the MMTV-*Neu* mice and genotyped by PCR, as previously described (9). *Neu* transgene was genotyped by quantitative real-time PCR under the following conditions: 95°C for 3 min, followed by 40 cycles (95°C for 20 s, 55°C for 30 s, and 72°C for 40 s). The following primers and probes were used for *Neu* amplification: forward primer, 5′-GCA TTG CTC CGC TGA GGC-3′; reverse primer, 5′-GCA GTG TCA ATG AGT ACG CGC C-3′; Taqman probe, 5′-/56-FAM/CC ATC CAA AGC AGG TCT CTG AGC TG/3BHQ-1/-3′.

Whole mount and histology

Mammary gland #4 was excised and used for morphologic analysis with whole mount mammary gland staining as described previously (6). Histologic analyses were performed to study changes in ductal epithelial cell morphology on the contralateral mammary gland #4 by fixing the gland in 10% formalin overnight, embedding in paraffin, mounting slices (5 μm) on glass slides, and staining with H&E.

Mammary gland and tumor primary epithelial cell culture

Epithelial cell cultures were generated as described previously (20). Briefly, mammary glands #1 to #5 (ages, 3 mo) and a portion of the tumors were removed from the mice and washed with PBS-50 μg/mL gentamicin (Invitrogen). Samples were minced, digested with 1 mg/mL of collagenase (Sigma-Aldrich), and incubated overnight at 37°C. The collagenase-treated and minced epithelial cell mixture was pelleted by centrifugation and washed with PBS. The pellet was resuspended and cultured for 4 h at 37°C in Ham's F12 medium (Invitrogen) supplemented with 10% fetal bovine serum, 4 μg/mL insulin (Invitrogen), 10 ng/mL EGF (Roche Applied Biosciences), 1 μg/mL hydrocortisone (Sigma-Aldrich), 50 μg/mL gentamicin (Invitrogen), and 1.5% penicillin/streptomycin. Supernatant cells were collected from the plates to avoid fibroblast contamination and replated for 5 d in the culture medium.

Western blotting and immunoprecipitation

Western blots and immunoprecipitations were performed with whole cell extracts from the primary mammary gland or mammary tumor cell cultures. Western blots were performed as described (11). For HER2/neu immunoprecipitations, 50 μg of mammary gland or tumor lysates were incubated with 5 μg of anti–ErbB-2/HER2 antibody and 40 μL of GammaBind G Sepharose beads overnight at 4°C with constant rotation. Immunoprecipitated samples were washed four times with lysis buffer and boiled at 95°C for 5 min. Western blot and immunoprecipitation analyses used the following antibodies: phosphorylated tyrosine clone 4G10, HER2/neu, p-HER3 (Upstate Biotechnology), β-actin (Chemicon), SRC-3 (Bethyl Laboratories), phosphorylated HER2/neu, phosphorylated AKT, phosphorylated p44/42 mitogen-activated protein kinase (MAPK; Thr^{202}/Tyr^{204}), MAPK, p54/p46 phosphorylated c-Jun NH_2 kinase (JNK; Thr^{183}/Tyr^{185}), JNK, cyclin E1 (Cell Signaling), and cyclin D1 (Neomarker). Protein band density was quantified by densitometry using Adobe Photoshop 7.0 software.

Immunohistochemistry

Immunohistochemical analyses were performed on mammary gland #4 and tumor sections, as previously described (6). All of the primary antibodies (mentioned above) were incubated overnight at 4°C and were diluted 1:100, except for the following: proliferating cell nuclear antigen (PCNA) clone PC10 (1:10,000; Sigma-Aldrich) and SRC-3 (1:200; Santa Cruz). Detection of both mouse and rabbit primary antibodies was performed using the DAKO Envision Plus HRP kit (DAKO Cytomation). Bound antibody was visualized using DAB substrate (Vector). The slides were counterstained with hematoxylin (Polysciences, Inc.).

Statistical analysis

χ^2 analysis was used to compare tumor multiplicity in the *Neu*/SRC-3^{wt} and *Neu*/SRC-3$^{+/-}$ mice. Kaplan-Meier analysis was used to evaluate tumor-free incidence. Statistical differences between tumor-free incidence curves for the *Neu*/SRC-3^{wt}, *Neu*/SRC-3$^{+/-}$, and *Neu*/SRC-3$^{-/-}$ mice were compared using the standard log-rank test. Statistical differences between the number of blood vessels per field for the *Neu*/SRC-3^{wt} and *Neu*/SRC-3$^{+/-}$ mice were compared using the Student's *t* test. A difference of $P < 0.05$ was considered to be statistically significant.

Results

SRC-3 regulates MMTV-*Neu* driven lateral side-branching in the mammary gland

Overexpression of *Neu* in the mouse is associated with extensive lateral side-branching, an abnormal mammary phenotype partly driven by increased growth factor signaling (21). Thus, we compared the preneoplastic mammary gland ductal morphology in female *Neu*/SRC-3^{wt}, *Neu*/SRC-3$^{+/-}$, and and *Neu*/SRC-3$^{-/-}$ mice at ages 3 to 4 months. Quantitative comparisons of the mammary gland whole mounts revealed a ~2-fold ($P < 0.001$) and ~8-fold ($P < 0.001$) decrease in lateral side-budding in the *Neu*/SRC-3$^{+/-}$ and *Neu*/SRC-3$^{-/-}$ mice, respectively (Fig. 1*A* and *C*). H&E-stained sections also showed comparable differences in lateral side-budding when SRC-3 levels were reduced in *Neu* mice (Fig. 1*A, bottom*).

Whole mount analysis at later stages of preneoplasia (ages, 6–7 months) revealed a considerable reduction (>60%, $P < 0.001$) of lateral side-budding in both the *Neu*/SRC-3$^{+/-}$ and *Neu*/SRC-3$^{-/-}$ mice relative to the *Neu*/SRC-3^{wt} mice (Fig. 1*B* and *C*). Consistent with previous reports using the SRC-3$^{-/-}$ mouse model, *Neu*/SRC-3$^{-/-}$ mice displayed decreased ductal branching (Fig. 1*A* and *B, right*), body weight, and mammary gland fat pad filling (data not shown; refs. 8, 9). Interestingly, none of these effects was observed in the *Neu*/SRC-3$^{+/-}$ mice. Of note is that the *Neu*/SRC3^{wt} and *Neu*/SRC3$^{+/-}$ mice displayed no observable differences in ductal branching from ages 3 to 7 months.

Reduced mammary gland hyperplasia and delayed tumorigenesis in *Neu* mice with lower SRC-3 levels

Next, we investigated the relevance of SRC-3 in *Neu*-driven hyperplasia and tumor formation. Relative to the *Neu*/SRC-3$^{+/-}$ mice, *Neu*/SRC-3^{wt} mice (ages, 9–12 months) displayed more extensive lateral side-budding and the formation of hyperplastic alveolar nodules in the mammary glands adjacent to the mammary tumors (Fig. 2*A*). The *Neu*/SRC-3$^{-/-}$ mice displayed no discernible preneoplastic changes (Fig. 2*A*).

The appearance of palpable mammary tumors is shown in a Kaplan-Meier plot of 25 *Neu*/SRC-3^{wt}, 23 *Neu*/SRC-3$^{+/-}$, and 14 *Neu*/SRC-3$^{-/-}$ mice (Fig. 2*B*). *Neu*/SRC-3^{wt} mice (77%) developed mammary tumors from 7 to 15 months, with a median age of 9 months. *Neu*/SRC-3$^{+/-}$ mice displayed a significant delay in tumor onset, with 70% of the mice developing mammary tumors from 15 to 24 months with a median age of 16 months. *Neu*/SRC-3$^{-/-}$ mice (100%) observed up to age of 24 months were protected from mammary tumor formation (Fig. 2*B*). Despite the delayed tumorigeneis in the *Neu*/SRC3$^{+/-}$ mice, there was no difference in the multiplicity of tumors per mouse (Fig. 2*B, bottom*). We also noted that *Neu*/SRC-3$^{+/-}$ tumors had large areas of necrotic tissue in all of the tumors examined ($n = 3$ mice; Fig. 2*C*). In contrast, all of the tumors from the *Neu*/SRC-3^{wt} mice displayed a noticeable increase in blood vessels when compared with the tumors from the *Neu*/SRC-3$^{+/-}$ mice ($n = 7$ mice; Fig. 2*C*). Relative to the *Neu*/SRC-3^{wt} mice, a ~25% ($P <$

0.05) reduction was observed in the average number of blood vessels per field in the *Neu*/SRC-3$^{+/-}$ mice (Fig. 2*C, bottom*).

Lower levels of SRC-3 reduce *Neu* phosphorylation in the preneoplastic mammary gland

To examine whether SRC-3 regulates the cellular levels or the activation of *Neu*, we measured *Neu* and phosphorylated *Neu* protein levels in preneoplastic mammary gland tissue samples. *Neu* and phosphorylated *Neu* levels were barely detectable in these samples using immunohistochemistry in mammary glands from *Neu*/SRC-3^{wt}, *Neu*/SRC-3$^{+/-}$, or *Neu*/SRC-3$^{-/-}$ mice (data not shown; Fig. 3*A*). These low levels of expression are consistent with the previous findings of DiGiovanna et al., who found undetectable immunohistochemical staining of phosphorylated *Neu* and *Neu* in normal mammary glands from MMTV-*Neu* mice (22). Therefore, to measure *Neu* and phosphorylated *Neu* expression levels in preneoplastic mammary glands, we generated primary mammary gland epithelial cell (MEC) cultures from the *Neu*/SRC-3^{wt}, *Neu*/SRC-3$^{+/-}$, and *Neu*/SRC-3$^{-/-}$ mice. Phosphorylated *Neu* levels in the preneoplastic MECs were significantly decreased in the *Neu*/SRC-3$^{+/-}$ and *Neu*/SRC-3$^{-/-}$ mice when compared with *Neu*/SRC-3^{wt} mice (Fig. 3*B, top*). However, total *Neu* protein levels were unchanged in MECs from *Neu*/SRC-3^{wt}, *Neu*/SRC-3$^{+/-}$, and *Neu*/SRC-3$^{-/-}$ mice (Fig. 3*B, middle*). Thus, the loss or lowering of SRC-3 levels does not affect the expressed levels of *Neu* in the mammary glands but does prevent activation of the *Neu* receptor.

Total SRC-3 levels were measured in MECs derived from the *Neu*/SRC-3^{wt}, *Neu*/SRC-3$^{+/-}$, and *Neu*/SRC-3$^{-/-}$ mice by immunohistochemistry and Western blot analysis. As expected, the SRC-3 levels were decreased by ~60% in the *Neu*/SRC-3$^{+/-}$ mice relative to *Neu*/SRC-3^{wt} mice (Fig. 3*C* and *D*) and SRC-3 expression was undetectable in the *Neu*/SRC-3$^{-/-}$ mice (Fig. 3*C* and *D*).

Decreased SRC-3 levels reduce *Neu* activation in mammary tumors

Because the overall levels of *Neu* remain unchanged in the preneoplastic MECs from the *Neu* mice (Fig. 3*A, middle*), we investigated the expression and phosphorylation of *Neu* in *Neu*/SRC-3^{wt} and *Neu*/SRC-3$^{+/-}$ mammary tumors (Fig. 4*A*). Consistent with previous reports, the *Neu*/SRC-3^{wt} tumors displayed high phosphorylated *Neu* expression (Fig. 4*A*; refs. 19, 22). In contrast, immunohistochemical analysis of *Neu*/SRC-3$^{+/-}$ tumors revealed a significant reduction (>60%, $P < 0.001$) in phosphorylated *Neu* levels (Fig. 4*A, bar graph*). To confirm these observations, we examined phosphorylated *Neu* levels in tumor epithelial cells cultured from *Neu*/SRC-3^{wt} and *Neu*/SRC-3$^{+/-}$ mice. *Neu*/SRC-3$^{+/-}$ mice displayed a ~80% reduction in phosphorylated *Neu* when compared with the *Neu*/SRC-3^{wt} tumor cells, despite comparable levels of total *Neu* in cells from both tumor types (Fig. 4*B*). Thus, the effect of SRC-3 reduction is primarily on the phosphorylation and not on the expression of *Neu* in mammary tumors.

We also determined the SRC-3 protein and mRNA expression levels in the *Neu*/SRC-3^{wt} and *Neu*/SRC-3$^{+/-}$ tumors. Immunohistochemical analyses of tumor sections from *Neu*/SRC-3$^{+/-}$ mice revealed a ~6-fold ($P < 0.001$) decrease in SRC-3 levels relative to the noticeably high levels of SRC-3 observed in the *Neu*/SRC3^{wt} tumors (Fig. 4*C*). Western blot analysis of tumor cell cultures from the *Neu*/SRC-3$^{+/-}$ mice showed a comparable 70% decrease of SRC-3 protein expression relative to the *Neu*/SRC3^{wt} cultures (Fig. 4*D*). SRC-3 mRNA expression was also assessed by *in situ* hybridization of tumor sections from both genotypes (Supplementary Fig. S1). SRC-3 mRNA levels were significantly decreased in the *Neu*/SRC-3$^{+/-}$ tumors relative to the *Neu*/SRC-3^{wt} tumors and absent in the nontumorigenic *Neu*/SRC-3$^{-/-}$ mice, thus correlating with the immunohistochemistry and Western blot results.

Decreased SRC-3 levels reduce epithelial cell proliferation

It has been well established that SRC-3 plays a significant role in growth factor–induced cell proliferation (7, 8, 10–12). Therefore, we asked whether the observed reduction of preneoplasia and tumorigenesis in *Neu* mice with reduced SRC-3 levels correlated with an overall decrease in cell proliferation. Cell proliferation in the mammary gland was measured through immunohistochemistry for nuclear expression of the mitosis marker, PCNA. The *Neu*/SRC-$3^{+/-}$ and *Neu*/SRC-$3^{-/-}$ mice displayed a significant decrease in PCNA expression relative to the *Neu*/SRC-3^{wt} mice (Fig. 5*A* and *C*). *Neu*/SRC-$3^{+/-}$ revealed a ~2-fold ($P < 0.001$) decrease in PCNA-positive cells relative to the *Neu*/SRC-3^{wt} tumors (Fig. 5*A* and *C*). In breast cancer, overexpression of the cell cycle regulatory genes, cyclin D1 and cyclin E, contribute significantly to cell cycle progression, mammary gland development, and tumor progression (24, 25). *Neu*/cyclin $D1^{-/-}$ mice display resistance to *Neu*-induced mammary tumorigenesis (25–27). Therefore, we analyzed cyclin D1 (Fig. 5*B* and *C*) and cyclin E (Fig. 5*D*) expression levels in our mouse model by immunohistochemistry and Western blot. MECs from *Neu*/SRC-$3^{+/-}$ mice at age of 3 months displayed a ~40% decrease in cyclin D1 and ~80% decrease in cyclin E levels relative to the *Neu*/SRC-3^{wt} mice (Fig. 5*D*). Consistent with these results, mammary glands at age of 6 months, as well as mammary tumors from *Neu* mice with reduced SRC-3 levels, displayed a ~4 fold ($P < 0.001$) decrease in cyclin D1 (Fig. 5*B–D*) and cyclin E levels (Fig. 5*D* and data not shown) relative to *Neu*/SRC-3^{wt} mice. Overall, these findings indicate that reduced SRC-3 levels in *Neu* mice delay tumor incidence by decreasing cell proliferation through the regulation of cell cycle proteins.

Regulation of phosphorylated extracellular signal-regulated kinase 1/2, p-JNK, p-AKT, and p-HER3 in *Neu*/SRC-3 mice

These data indicate that SRC-3 plays a rate-limiting role in the progression of *Neu*-induced preneoplasia and mammary tumorigenesis. We therefore determined which *Neu*-dependent mitogenic kinase pathways are down-regulated during mammary tumorigenesis in *Neu* overexpressing mice with reduced SRC-3 levels. We and other groups have linked SRC-3–driven cancer progression with changes in extracellular signal-regulated kinase 1/2 (ERK1/2), JNK, and AKT signaling (7, 11, 12, 23). Activation of the ERK1/2 pathway upon growth factor or hormone stimulation leads to the subsequent transactivation of SRC-3 in MCF-7 breast cancer cells (23). Shou et al. observed in MCF-7/HER2-18 cells that the HER2 pathway phosphorylates ERK1/2, which subsequently activates SRC-3 (16). Thus, we examined how ERK1/2 signaling was affected in mice with reduced SRC-3 levels during *Neu*-induced tumorigenesis. Immunohistochemical analysis of *Neu*/SRC-$3^{+/-}$ and *Neu*/SRC-$3^{-/-}$ mice at the age of 6 months displayed >2-fold ($P < 0.001$) reduction in p-ERK1/2 levels relative to the *Neu*/SRC-3^{wt} mice (Fig. 6*A* and *C*). Western blot analysis of p-ERK1/2 in *Neu*/SRC-$3^{+/-}$ mice at age of 3 months displayed a ~60% reduction in p-ERK1/2 levels relative to *Neu*/SRC-3^{wt} mice (Fig. 6*D*). Interestingly, immunohistochemistry and Western blot analysis of tumors overexpressing *Neu* showed low p-ERK1/2 and total ERK levels relative to those seen at earlier time points (Fig. 6*A, C*, and *D*).

We measured levels of p-JNK, another MAPK family member, in mammary tumorigenesis. Mammary gland tissue sections from *Neu* mice with deficient SRC-3 levels (ages, 3 and 6 months) displayed a significant decrease in p-JNK levels (Fig. 6*A, C*, and *D*). *Neu*/SRC-$3^{+/-}$ tumor samples showed a drastic 70% reduction in the activation of JNK relative to *Neu*/SRC-3^{wt} tumors (Fig. 6*D*).

It is widely accepted that SRC-3 plays a critical role in phosphatidylinositol 3-kinase (PI3K)/AKT signaling in mammary tumorigenesis (7, 11). Interestingly, we observed almost undetectable levels of AKT activation in the preneoplastic mammary glands at ages of 3 and 6 months (data not shown; Fig. 6*D*). Consistent with these results, we were also unable to

detect p-AKT levels in early preneoplasia by immunohistochemical analysis (data not shown). However, p-AKT levels were noticeably increased in *Neu* tumors with wild-type SRC-3 expression, but down-regulated in tumors with reduced SRC-3 levels (Fig. 6*D*). MECs from *Neu*/SRC-$3^{+/-}$ tumors displayed a ~90% decrease in p-AKT levels relative to *Neu*/SRC-3^{wt} tumors. Total AKT levels were comparable between preneoplastic and neoplastic cells from *Neu*/SRC-3^{wt} and *Neu*/SRC-$3^{+/-}$ mice. We also observed an overall increase in total AKT expression in the neoplastic lesions. Taken together, this implies that AKT protein expression is unaffected by SRC-3 levels, but AKT activation is regulated by SRC-3. We also observed a reduction in p-HER3 levels in the *Neu*/SRC-$3^{+/-}$ mice relative to the *Neu*/SRC-3^{wt} mice in the primary tumor epithelial cell extracts (Fig. 6*D*). Similar to the p-AKT levels before tumor formation, the phosphorylation of HER3 was undetectable in preneoplastic primary epithelial cell extracts (ages, 3 months; Fig. 6*D*). Thus, the activation of AKT is most likely through the activation of HER2/*neu* and cross-talk with p-HER3.

Discussion

In this study, we show a pivotal role for SRC-3 in HER2/*Neu*-induced mammary tumorigenesis. At all stages of preneoplasia and neoplasia, we determined that loss of one allele of SRC-3 in mice delayed tumorigenesis and reduced *Neu*-induced subcellular signaling in the mammary epithelium (summarized in Supplementary Fig. S2). SRC-3 has variable roles in oncogenesis; it has been shown that the loss of SRC-3 in mice drives the development of malignant B-cell lymphomas (28). In contrast, loss of SRC-3 in the TRAMP prostate cancer mouse model predominantly affected only late-stage neoplasia (29). These results suggest that the loss of SRC-3 expression can have varied effects on the carcinogenic process depending on the tissue site and the oncogene driving tumorigenesis. Of major relevance for breast cancer, HER2/*neu*–driven mammary carcinogenesis is dependent on endogenous SRC-3. This gives mechanistic relevance to earlier correlative observations between high levels of SRC-3 and HER2/*neu* expression and the development of antiestrogen resistance in human breast cancers (15, 16, 30). Our data argues that, *in vivo*, SRC-3 is downstream of the activated HER2/*neu* receptor and is required to maintain the full tumorigenic potential of the HER2/*neu* oncogene.

An unexpected observation was the increased expression of SRC-3 in *Neu*-induced mammary tumors relative to the normal adjacent mammary tissue. This suggests a positive feedback loop, whereby activated *Neu* drives the expression and activation of SRC-3, subsequently potentiating greater *Neu* signaling. Consistent with this feedback model, high levels of phosphorylated *Neu* were observed in the *Neu*-induced tumors. Also consistent with this model, reduced levels of SRC-3 in the *Neu*/SRC-$3^{+/-}$ mice decreased the activation of phosphorylated *Neu*. Likewise, activation of HER3 is down-regulated in the *Neu*/SRC-$3^{+/-}$ tumors, without changing the total HER3 protein levels. These latter results are reminiscent of an effect we observed previously, wherein the reduction of SRC-3 *in vitro* reduced EGF-induced phosphorylation of EGFR (HER1), partially through changes in cellular phosphatase activity (12). We speculate that the chronic reduction of SRC-3 in the *Neu*/SRC-$3^{+/-}$ and *Neu*/SRC-$3^{-/-}$ mice regulates the activation of the HER family of receptors possibly through influencing HER receptor dimerization, through receptor internalization, or through an enzyme that controls receptor phosphorylation. Whatever the mechanism of reduced HER receptor activation, the net result of lowering SRC3 levels in the mammary epithelium is a profound loss of HER2/*neu* signaling in the tumors.

The PI3K/AKT pathway is known to have prognostic value in human breast cancers and is a common downstream target of HER2/*neu* and SRC-3–driven mammary neoplasia (7, 27, 31). Clinical data has delineated a critical role for the PI3K/AKT pathway in causing resistance to trastuzumab in breast cancer patients (32, 33). Overexpression of SRC-3 in

mice increases p-AKT levels in tissues that develop preneoplastic changes and tumors (7). HER2/*neu* also signals through the PI3K/AKT pathway mediating cell proliferation through cyclin D1 in mammary cancer (31, 34, 35). It has been reported that in early preneoplastic mammary gland lesions, low levels of ErbB2 are correlated with low levels of p-AKT (35) and, as neoplasia progresses, increased ErbB2 expression results in the subsequent increase in p-AKT levels (35). Similarly, in our studies, we found low levels of p-AKT during the preneoplastic stages (3–6 months) of tumorigenesis. AKT protein levels were increased in the *Neu*/SRC3^{wt} tumors, but the phosphorylation of AKT was nevertheless reduced in the *Neu*/SRC-3$^{+/-}$ mice. There is growing evidence that the coexpression of HER2/*neu* and HER3 plays a critical role in the activation of the PI3K/AKT pathway in human and mouse neoplasia (36, 37). In this regard, we also observed an increase in p-HER3 in *Neu*/SRC-3^{wt} tumors, whereas it was significantly decreased in the *Neu*/SRC-3$^{+/-}$ tumors. Taken together, lower levels of activated *Neu* in conjunction with reduced levels of p-HER3 may play a major role in reducing tumorigenesis in the *Neu*/SRC3$^{+/-}$ mice via reduced AKT signaling.

In addition to the PI3K/AKT pathway, we also found that JNK signaling was significantly reduced in the *Neu*/SRC3$^{+/-}$ mammary tumors. Increased JNK signaling has been correlated with proliferation and oncogenesis in various transformed cell lines. For instance, recent studies by our group found that the SRC-3 siRNA decreased EGF-driven JNK phosphorylation and cell proliferation in several transformed epithelial cell lines (12). In human breast cancer cells, the inhibition of JNK activity reduced *Neu*T-induced cyclin D1 promotor activity (27). In contrast to AKT and JNK, our results suggest that the MAPK pathway is activated early in preneoplasia and then the activation mechanism through *Neu* is lost in the later stages of tumorigenesis. This pattern of MAPK activation differs from previous reports that have indicated that MAPK is activated at high levels in HER2/*neu*–positive tumors (38). However, our findings in the MEC cultures reflect only what is happening in the epithelial compartment of the mammary gland, whereas most previous signaling data have been derived from homogenized tumor lysates that are from epithelial and stromal compartments of the tumor. Importantly, for all the *Neu*-induced signaling pathways examined in this study, we found that the level of activation of the signaling molecules is decreased by reducing the levels of SRC-3 in the *Neu*/SRC3$^{+/-}$ mice. This suggests that some unifying upstream event is turned off for all the pathways, thus attenuating the amplitude of most of the *Neu*-dependent kinase signaling pathways. Although the phosphorylation of HER2/*neu*, HER1/EGFR, or HER3 is likely to be the rate-limiting points of control for SRC-3, it is also possible that other upstream signaling molecules are controlled by the levels of SRC-3 in the mammary epithelial cells.

SRC-3 has been shown to be rate-limiting for ER and PR signaling in breast cancer cells (1, 39). However, these receptors are unlikely to be mediating the effect of SRC-3 in the current studies because the MMTV-*Neu* model is considered to be ER negative, similar to human breast cancer (40), and cDNA array analysis of gene expression in these tumors found no evidence of estrogen-induced gene expression patterns (41). We cannot entirely rule out an effect through the low levels of ER present in these tumors at some stage of tumorigenesis. Loss of ER in MMTV-*Neu* mice does increase the time to tumor formation; however, *Neu*/ER$^{-/-}$ mice, with total loss of ER, still developed mammary tumors (42). In contrast, *Neu*/SRC-3$^{-/-}$ mice did not develop any tumors during the 24 months of this study, indicating that these models are not equivalent, and SRC-3 has effects in addition to its role in ER signaling. Indeed, the profound loss of ductal development and lateral branching in SRC3$^{-/-}$ mice suggest that a progenitor cell for tumorigenesis may well be lost in these mice. In contrast, the reduction of SRC-3 levels in the *Neu*/SRC3$^{+/-}$ mammary epithelial cells does not reduce the total number of ducts suggesting that ductal progenitor cells still develop. Therefore, the reduced lateral side-budding branching in *Neu*/SRC3$^{+/-}$ mice is most likely through reduced activation of *Neu* and its subsequent downstream growth factor signaling.

In mice with reduced SRC-3 expression, there is a significant decrease in epithelial proliferation that is most likely caused by the reductions in cyclin D1 and cyclin E protein expression that we observed. *Neu*-induced mammary adenocarcinoma proliferation requires the expression of cyclin D1 and its cross-talk with cyclin E. *Neu*/cyclin $D1^{-/-}$ mice display resistance to mammary gland tumorigenesis (25–27); although of note is that 35% of *Neu*/cyclin $D1^{-/-}$ mice can develop mammary tumors due to a compensatory increase in cyclin E levels (43). Furthermore, trastuzumab, a monoclonal antibody that targets ErbB2/HER2 in human breast cancer therapy, can cause decreased cyclin E kinase activity (44). Relevant to the current study are reports that cyclin D1 also plays a significant role in SRC-3–driven tumorigenesis, (45, 46), suggesting that *Neu* regulation of SRC-3 and cyclin D1 may be connected. Collectively, these results provide evidence that the reduction of SRC-3 in mice overexpressing *Neu* delays tumor incidence by impinging on the activity of cell cycle proteins and decreasing cell proliferation.

The histologic differences in the mammary tumors that develop in the *Neu*/$SRC3^{+/-}$ versus *Neu*/$SRC3^{wt}$ mice are of potential significance. The *Neu*/$SRC3^{+/-}$ tumors displayed areas that were highly necrotic, whereas the MMTV-*Neu* tumors were highly vascularized. Increased angiogenesis drives breast cancer tumorigenesis and is directly correlated to the severity of tumorigenesis. Vascular endothelial growth factor, a signaling protein involved in angiogenesis, is known to accelerate the incidence of mammary tumors in *Neu*-driven tumorigenesis (47). Fibroblast growth factor binding protein, another angiogenic factor, is regulated by SRC-3 (12, 48). Our data suggest that SRC-3 may play a role in tumor maintenance by regulating angiogenesis and the rate of necrosis in *Neu*-induced tumors, and this may contribute to the tumor latency in the *Neu*/$SRC3^{+/-}$ mice.

Finally, it should be noted that the overexpression of AIB1/SRC-3 alone can produce tumors in the mouse mammary gland and is correlated with the potentiation of IGF-I signaling (7). At lower levels of SRC-3 expression, hyperplasia and preneoplasia are observed and also correlated with potentiation of the IGF-I signaling pathway (6, 49). Interestingly, none of these previous studies examined the role of the HER family of oncogenic receptors. We now describe a positive feedback loop between SRC-3 and HER2/*neu* that could provide an additional route to oncogenesis in these animals.

In conclusion, we have shown that SRC-3 plays a major role in *Neu*-induced preneoplastic phenotypic changes and signaling, such as AKT and JNK activation and tumorigenesis in the mammary gland of mice. Only a 50% reduction in SRC-3 levels in the mammary epithelium can delay HER2/*neu*–driven tumorigenesis and reduce the total number of tumors that develop. In addition, the reduction in SRC-3 may reduce the angiogenesis in the tumors. Our results emphasize that targeting endogenous SRC-3 could provide greater efficacy to the current therapies used to treat tumors overexpressing HER2/*Neu*.

Supplementary Material

Refer to Web version on PubMed Central for supplementary material.

Acknowledgments

Grant support: National Cancer Institute grants CA11677 and CA108441 (A.T. Riegel), Department of Defense Predoctoral grant BC050151 (M.P. Fereshteh), and Susan G. Komen Cancer Foundation Postdoctoral grant PDF0503642 (M.T. Tilli).

We thank Amy Hapip who assisted with the quantification of whole mount and immunohistochemical analyses.

References

1. Anzick SL, Kononen J, Walker RL, et al. AIB1, a steroid receptor coactivator amplified in breast and ovarian cancer. Science. 1997; 277:965–8. [PubMed: 9252329]
2. List HJ, Reiter R, Singh B, Wellstein A, Riegel AT. Expression of the nuclear coactivator AIB1 in normal and malignant breast tissue. Breast Cancer Res Treat. 2001; 68:21–8. [PubMed: 11678305]
3. Gnanapragasam VJ, Leung HY, Pulimood AS, Neal DE, Robson CN. Expression of RAC 3, a steroid hormone receptor coactivator in prostate cancer. Br J Cancer. 2001; 85:1928–36. [PubMed: 11747336]
4. Bautista S, Valles H, Walker RL, et al. In breast cancer, amplification of the steroid receptor coactivator gene AIB1 is correlated with estrogen and progesterone receptor positivity. Clin Cancer Res. 1998; 4:2925–9. [PubMed: 9865902]
5. Reiter R, Wellstein A, Riegel AT. An isoform of the coactivator AIB1 that increases hormone and growth factor sensitivity is overexpressed in breast cancer. J Biol Chem. 2001; 276:39736–41. [PubMed: 11502741]
6. Tilli MT, Reiter R, Oh AS, et al. Overexpression of an N-terminally truncated isoform of the nuclear receptor coactivator amplified in breast cancer 1 leads to altered proliferation of mammary epithelial cells in transgenic mice. Mol Endocrinol. 2005; 19:644–56. [PubMed: 15550471]
7. Torres-Arzayus MI, Font de Mora J, Yuan J, et al. High tumor incidence and activation of the PI3K/AKT pathway in transgenic mice define AIB1 as an oncogene. Cancer Cell. 2004; 6:263–74. [PubMed: 15380517]
8. Wang Z, Rose DW, Hermanson O, et al. Regulation of somatic growth by the p160 coactivator p/CIP. Proc Natl Acad Sci U S A. 2000; 97:13549–54. [PubMed: 11087842]
9. Xu J, Liao L, Ning G, Yoshida-Komiya H, Deng C, O'Malley BW. The steroid receptor coactivator SRC-3 (p/CIP/RAC3/AIB1/ACTR/TRAM-1) is required for normal growth, puberty, female reproductive function, and mammary gland development. Proc Natl Acad Sci U S A. 2000; 97:6379–84. [PubMed: 10823921]
10. Kuang SQ, Liao L, Zhang H, Lee AV, O'Malley BW, Xu J. AIB1/SRC-3 deficiency affects insulin-like growth factor I signaling pathway and suppresses v-Haras-induced breast cancer initiation and progression in mice. Cancer Res. 2004; 64:1875–85. [PubMed: 14996752]
11. Oh A, List HJ, Reiter R, et al. The nuclear receptor coactivator AIB1 mediates insulin-like growth factor I-induced phenotypic changes in human breast cancer cells. Cancer Res. 2004; 64:8299–308. [PubMed: 15548698]
12. Lahusen T, Fereshteh M, Oh A, Wellstein A, Riegel AT. Epidermal growth factor receptor tyrosine phosphorylation and signaling controlled by a nuclear receptor coactivator, amplified in breast cancer 1. Cancer Res. 2007; 67:7256–65. [PubMed: 17671194]
13. Slamon DJ, Clark GM, Wong SG, Levin WJ, Ullrich A, McGuire WL. Human breast cancer: correlation of relapse and survival with amplification of the HER-2/neu oncogene. Science. 1987; 235:177–82. [PubMed: 3798106]
14. Bouras T, Southey MC, Venter DJ. Overexpression of the steroid receptor coactivator AIB1 in breast cancer correlates with the absence of estrogen and progester-one receptors and positivity for p53 and HER2/neu. Cancer Res. 2001; 61:903–7. [PubMed: 11221879]
15. Osborne CK, Bardou V, Hopp TA, et al. Role of the estrogen receptor coactivator AIB1 (SRC-3) and HER-2/neu in tamoxifen resistance in breast cancer. J Natl Cancer Inst. 2003; 95:353–61. [PubMed: 12618500]
16. Shou J, Massarweh S, Osborne CK, et al. Mechanisms of tamoxifen resistance: increased estrogen receptor-HER2/neu cross-talk in ER/HER2-positive breast cancer. J Natl Cancer Inst. 2004; 96:926–35. [PubMed: 15199112]
17. Kirkegaard T, McGlynn LM, Campbell FM, et al. Amplified in breast cancer 1 in human epidermal growth factor receptor-positive tumors of tamoxifen-treated breast cancer patients. Clin Cancer Res. 2007; 13:1405–11. [PubMed: 17332282]
18. Siegel PM, Dankort DL, Hardy WR, Muller WJ. Novel activating mutations in the neu protooncogene involved in induction of mammary tumors. Mol Cell Biol. 1994; 14:7068–77. [PubMed: 7935422]

19. Guy CT, Webster MA, Schaller M, Parsons TJ, Cardiff RD, Muller WJ. Expression of the neu protooncogene in the mammary epithelium of transgenic mice induces metastatic disease. Proc Natl Acad Sci U S A. 1992; 89:10578–82. [PubMed: 1359541]
20. Wulf G, Garg P, Liou YC, Iglehart D, Lu KP. Modeling breast cancer *in vivo* and *ex vivo* reveals an essential role of Pin1 in tumorigenesis. EMBO J. 2004; 23:3397–407. [PubMed: 15257284]
21. Andrechek ER, Hardy WR, Siegel PM, Rudnicki MA, Cardiff RD, Muller WJ. Amplification of the neu/erbB-2 oncogene in a mouse model of mammary tumorigenesis. Proc Natl Acad Sci U S A. 2000; 97:3444–9. [PubMed: 10716706]
22. DiGiovanna MP, Lerman MA, Coffey RJ, Muller WJ, Cardiff RD, Stern DF. Active signaling by *Neu* in transgenic mice. Oncogene. 1998; 17:1877–84. [PubMed: 9778054]
23. Font de Mora J, Brown M. AIB1 is a conduit for kinase-mediated growth factor signaling to the estrogen receptor. Mol Cell Biol. 2000; 20:5041–7. [PubMed: 10866661]
24. Geng Y, Yu Q, Sicinska E, et al. Cyclin E ablation in the mouse. Cell. 2003; 114:431–43. [PubMed: 12941272]
25. Yu Q, Geng Y, Sicinski P. Specific protection against breast cancers by cyclin D1 ablation. Nature. 2001; 411:1017–21. [PubMed: 11429595]
26. Landis MW, Pawlyk BS, Li T, Sicinski P, Hinds PW. Cyclin D1-dependent kinase activity in murine development and mammary tumorigenesis. Cancer Cell. 2006; 9:13–22. [PubMed: 16413468]
27. Lee RJ, Albanese C, Fu M, et al. Cyclin D1 is required for transformation by activated *Neu* and is induced through an E2F-dependent signaling pathway. Mol Cell Biol. 2000; 20:672–83. [PubMed: 10611246]
28. Coste A, Antal MC, Chan S, et al. Absence of the steroid receptor coactivator-3 induces B-cell lymphoma. EMBO J. 2006; 25:2453–64. [PubMed: 16675958]
29. Chung AC, Zhou S, Liao L, Tien JC, Greenberg NM, Xu J. Genetic ablation of the amplified-in-breast cancer 1 inhibits spontaneous prostate cancer progression in mice. Cancer Res. 2007; 67:5965–75. [PubMed: 17575167]
30. Osborne CK, Schiff R. Growth factor receptor crosstalk with estrogen receptor as a mechanism for tamoxifen resistance in breast cancer. Breast. 2003; 12:362–7. [PubMed: 14659106]
31. Hutchinson JN, Jin J, Cardiff RD, Woodgett JR, Muller WJ. Activation of Akt-1 (PKB-a) can accelerate ErbB-2-mediated mammary tumorigenesis but suppresses tumor invasion. Cancer Res. 2004; 64:3171–8. [PubMed: 15126356]
32. Berns K, Horlings HM, Hennessy BT, et al. A Functional Genetic Approach Identifies the PI3K Pathway as a Major Determinant of Trastuzumab Resistance in Breast Cancer. Cancer Cell. 2007; 12:395–402. [PubMed: 17936563]
33. Nagata Y, Lan KH, Zhou X, et al. PTEN activation contributes to tumor inhibition by trastuzumab, and loss of PTEN predicts trastuzumab resistance in patients. Cancer Cell. 2004; 6:117–27. [PubMed: 15324695]
34. Ju X, Katiyar S, Wang C, et al. Akt1 governs breast cancer progression *in vivo*. Proc Natl Acad Sci U S A. 2007; 104:7438–43. [PubMed: 17460049]
35. Zhou X, Tan M, Stone Hawthorne V, et al. Activation of the Akt/mammalian target of rapamycin/4E-BP1 pathway by ErbB2 overexpression predicts tumor progression in breast cancers. Clin Cancer Res. 2004; 10:6779–88. [PubMed: 15501954]
36. Holbro T, Beerli RR, Maurer F, Koziczak M, Barbas CF III, Hynes NE. The ErbB2/ErbB3 heterodimer functions as an oncogenic unit: ErbB2 requires ErbB3 to drive breast tumor cell proliferation. Proc Natl Acad Sci U S A. 2003; 100:8933–8. [PubMed: 12853564]
37. Siegel PM, Ryan ED, Cardiff RD, Muller WJ. Elevated expression of activated forms of *Neu*/ErbB-2 and ErbB-3 are involved in the induction of mammary tumors in transgenic mice: implications for human breast cancer. EMBO J. 1999; 18:2149–64. [PubMed: 10205169]
38. Schade B, Lam SH, Cernea D, et al. Distinct ErbB-2 coupled signaling pathways promote mammary tumors with unique pathologic and transcriptional profiles. Cancer Res. 2007; 67:7579–88. [PubMed: 17699761]

39. Suen CS, Berrodin TJ, Mastroeni R, Cheskis BJ, Lyttle CR, Frail DE. A transcriptional coactivator, steroid receptor coactivator-3, selectively augments steroid receptor transcriptional activity. J Biol Chem. 1998; 273:27645–53. [PubMed: 9765300]
40. Wu K, Zhang Y, Xu XC, et al. The retinoid X receptor-selective retinoid, LGD1069, prevents the development of estrogen receptor-negative mammary tumors in transgenic mice. Cancer Res. 2002; 62:6376–80. [PubMed: 12438218]
41. Herschkowitz JI, Simin K, Weigman VJ, et al. Identification of conserved gene expression features between murine mammary carcinoma models and human breast tumors. Genome Biol. 2007; 8:R76. [PubMed: 17493263]
42. Hewitt SC, Bocchinfuso WP, Zhai J, et al. Lack of ductal development in the absence of functional estrogen receptor a delays mammary tumor formation induced by transgenic expression of ErbB2/neu. Cancer Res. 2002; 62:2798–805. [PubMed: 12019156]
43. Bowe DB, Kenney NJ, Adereth Y, Maroulakou IG. Suppression of *Neu*-induced mammary tumor growth in cyclin D1 deficient mice is compensated for by cyclin E. Oncogene. 2002; 21:291–8. [PubMed: 11803472]
44. Lane HA, Beuvink I, Motoyama AB, Daly JM, Neve RM, Hynes NE. ErbB2 potentiates breast tumor proliferation through modulation of p27(Kip1)-Cdk2 complex formation: receptor overexpression does not determine growth dependency. Mol Cell Biol. 2000; 20:3210–23. [PubMed: 10757805]
45. Louie MC, Revenko AS, Zou JX, Yao J, Chen HW. Direct control of cell cycle gene expression by protooncogene product ACTR, and its autoregulation underlies its transforming activity. Mol Cell Biol. 2006; 26:3810–23. [PubMed: 16648476]
46. Louie MC, Zou JX, Rabinovich A, Chen HW. ACTR/AIB1 functions as an E2F1 coactivator to promote breast cancer cell proliferation and antiestrogen resistance. Mol Cell Biol. 2004; 24:5157–71. [PubMed: 15169882]
47. Oshima RG, Lesperance J, Munoz V, et al. Angiogenic acceleration of *Neu* induced mammary tumor progression and metastasis. Cancer Res. 2004; 64:169–79. [PubMed: 14729621]
48. Harris VK, Coticchia CM, Kagan BL, Ahmad S, Wellstein A, Riegel AT. Induction of the angiogenic modulator fibroblast growth factor-binding protein by epidermal growth factor is mediated through both MEK/ERK and p38 signal transduction pathways. J Biol Chem. 2000; 275:10802–11. [PubMed: 10753873]
49. Avivar A, Garcia-Macias MC, Ascaso E, Herrera G, O'Connor JE, de Mora JF. Moderate overexpression of AIB1 triggers pre-neoplastic changes in mammary epithelium. FEBS Lett. 2006; 580:5222–6. [PubMed: 16963027]

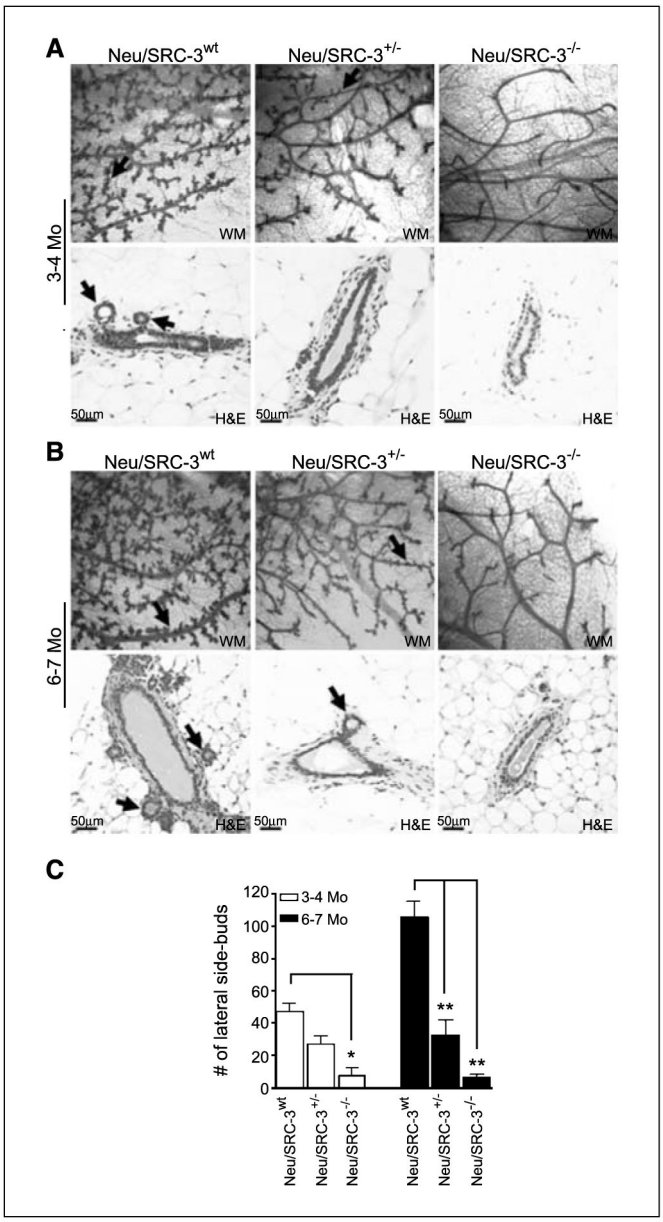

Figure 1.

Decreased mammary gland lateral side-budding in female MMTV-*Neu* mice with reduced levels of SRC-3. *A* and *B,* representative mammary gland (*MG*) whole mount (*WM*; magnification, 4×; *top*) and H&E (magnification, 20×; *bottom*) stained tissue sections from mice at ages of 3 to 4 mo (*A*) and 6 to 7 mo (*B*). The data are representative of mammary glands taken from four mice from each genotype. *Black arrows,* lateral side-budding in whole mount and H&E-stained sections. *C,* quantification of lateral side-budding along the mammary gland ducts. The number of lateral side buds was counted from 10 fields per whole mount from each mouse (magnification, 10×). *Columns,* mean; *bars,* SD ($n = 4$ mice from each genotype). *, $P < 0.05$ and **, $P < 0.001$, one-way ANOVA.

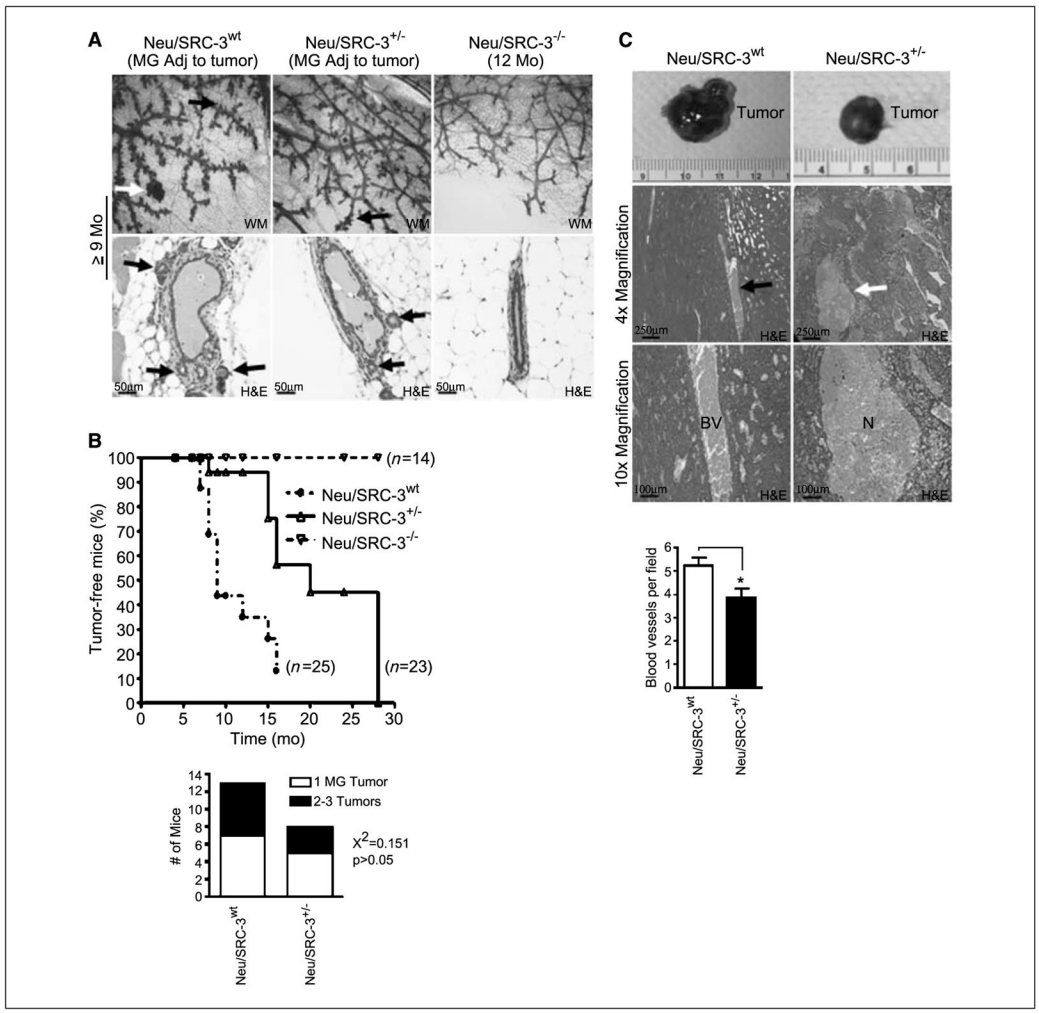

Figure 2.

Reduced SRC-3 levels in MMTV-*Neu* mice increase the latency of *Neu*-driven mammary tumorigenesis. *A,* representative mammary gland whole mounts (magnification, 10×; *top*) and H&E (magnification, 20×; *bottom*) stained tissue sections from mammary glands adjacent to tumors from *Neu*/SRC-3^{wt}, *Neu*/SRC-3$^{+/-}$, and *Neu*/SRC-3$^{-/-}$ mice. The data is representative of four mice examined from each genotype. *Black arrows,* lateral side-budding; *white arrow,* presence of a typical hyperplastic alveolar nodule (*top*). *B, top,* Kaplan-Meier analysis of tumor-free incidence comparing *Neu*/SRC-3^{wt} with the *Neu*/SRC-3$^{+/-}$ and *Neu*/SRC-3$^{-/-}$ mice. *Bottom,* quantification of the number of tumors per mouse from *Neu*/SRC-3$^{+/-}$ (n = 8) and *Neu*/SRC-3$^{-/-}$ mice (n = 13) was analyzed using χ^2 test. *C,* photographs showing representative primary mammary tumors harvested from *Neu*/SRC-3^{wt} (9 mo of age) and *Neu*/SRC-3$^{+/-}$ (19 mo of age) mice (*top*). Representative paraffin-embedded H&E-stained mammary tumors [magnification, 4× (*middle*) and 10× (*bottom*)] from *Neu*/SRC-3^{wt} (n = 7 mice analyzed) and *Neu*/SRC-3$^{+/-}$ mice (n = 3 mice analyzed). Representative blood vessels (*BV; left*). Representative areas of necrosis (*N; right*). The bar chart represents the quantification of the number of blood vessels per field in tumors from the *Neu*/SRC-3^{wt} (n = 8) and *Neu*/SRC-3$^{+/-}$ (n = 3) mice. Ten fields were counted per mouse (magnification, 40×). *Columns,* mean; *bars,* SD. *, $P < 0.05$, Student's t test.

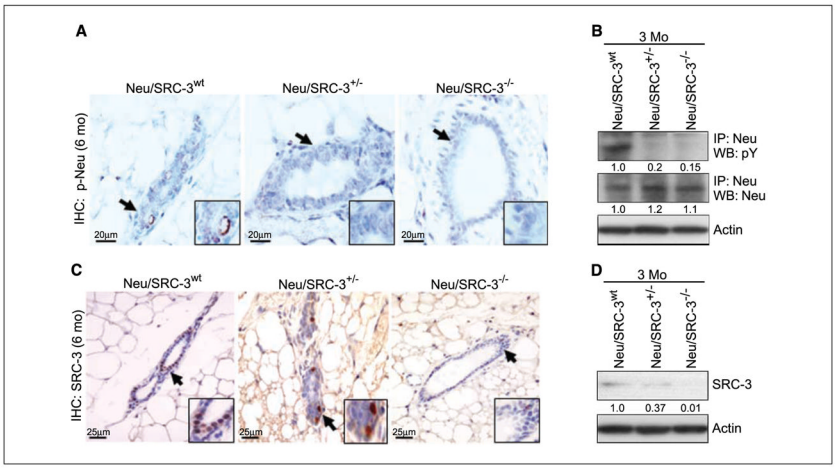

Figure 3.

Relative expression levels of *Neu*, phosphorylated *Neu* (*p-Neu*), and SRC-3 in primary mammary epithelial cells and tissue sections. *A,* representative immunohistochemical (*IHC*) analyses of phosphorylated *Neu* levels in mammary gland #4 of *Neu*/SRC-3^{wt}, *Neu*/SRC-$3^{+/-}$, and *Neu*/SRC-$3^{-/-}$ mice 6 mo of age (magnification, 60×). The black arrows and magnified region is representative of epithelial cell staining for phosphorylated *Neu. B,* total levels of *Neu* and phosphorylated *Neu* were immunoprecipitated and Western blotted from primary MEC lysates from mice at 3 mo of age. *C,* representative immunohistochemical analysis of SRC-3 expression in preneoplastic mammary gland tissue sections taken from mice at 6 mo of age. *Arrows,* mammary ductal epithelial cells staining positive for SRC-3 expression (magnification, 40×). *D,* mammary glands were harvested and cultured from mice 3 mo of age. Western blot analysis was performed on whole cell extracts from MEC cultures to determine the relative SRC-3 expression levels from the indicated genotypes. Data are representative of at least two independent experiments using the mammary glands of two to three mice from each genotype. Densitometry values represent phosphorylated *Neu, Neu*, and SRC-3 band intensities normalized to total actin.

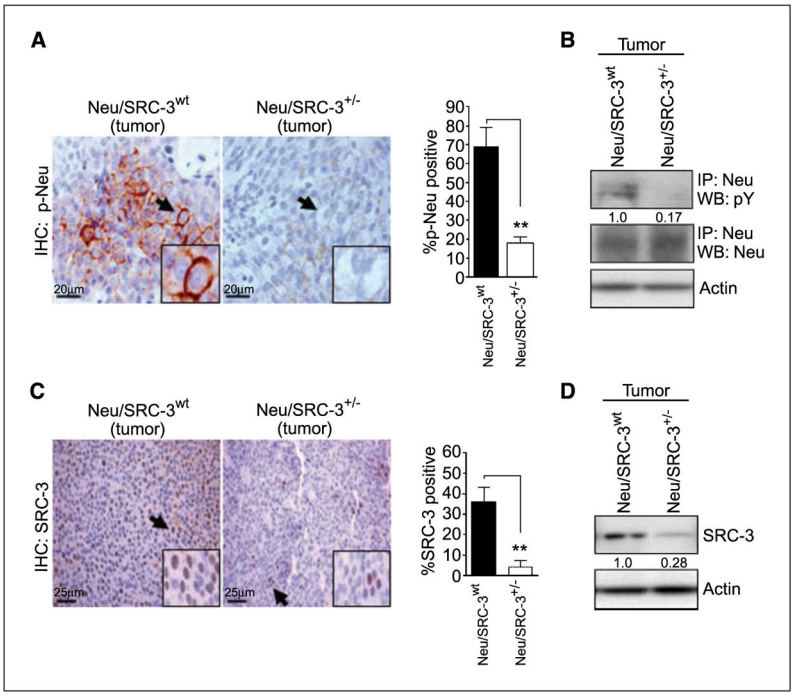

Figure 4.

SRC-3 levels determine the phosphorylation of *Neu* in mammary tumors. *A,* tumors from *Neu*/SRC-3^{wt} and *Neu*/SRC-3$^{+/-}$ mice were excised and paraffin-embedded. Immunohistochemistry was used to assess phosphorylated *Neu* levels in both *Neu*/SRC-3^{wt} and *Neu*/SRC-3$^{+/-}$ tumors (magnification, 60×). The bar charts represent the quantification of phosphorylated *Neu* staining; 100 cells were counted per field, and 10 fields were counted per mouse (magnification, 60×). *Columns,* mean of three independent experiments; *bars,* SD ($n = 3$ mice from each indicated genotype). **, $P < 0.001$, one-way ANOVA. *B,* primary tumor cells were cultured from *Neu*/SRC-3^{wt} and *Neu*/SRC-3$^{+/-}$ mice with mammary tumors. Immunoprecipitation for *Neu* was performed on whole cell extracts. Western blot analysis for phosphorylated *Neu*, and total *Neu* was performed on the immunoprecipitated products. *C,* paraffin-embedded tumor sections were used for the immunohistochemical detection of SRC-3 (magnification, 40×). *Arrows,* tumor cells that stained positive for SRC-3. The bar charts represent the quantification of SRC-3 staining; 100 cells were counted per field, and 10 fields were counted per genotype (magnification, 40×). *Columns,* mean of four independent experiments; *bars,* SD ($n = 4$ mice from each indicated genotype). **, $P < 0.001$, one-way ANOVA. *D,* representative SRC-3 Western blot analysis of whole cell protein extracts from primary tumor cell cultures. Densitometry values (*B* and *D*) represent phosphorylated *Neu* or SRC-3 levels normalized to total actin.

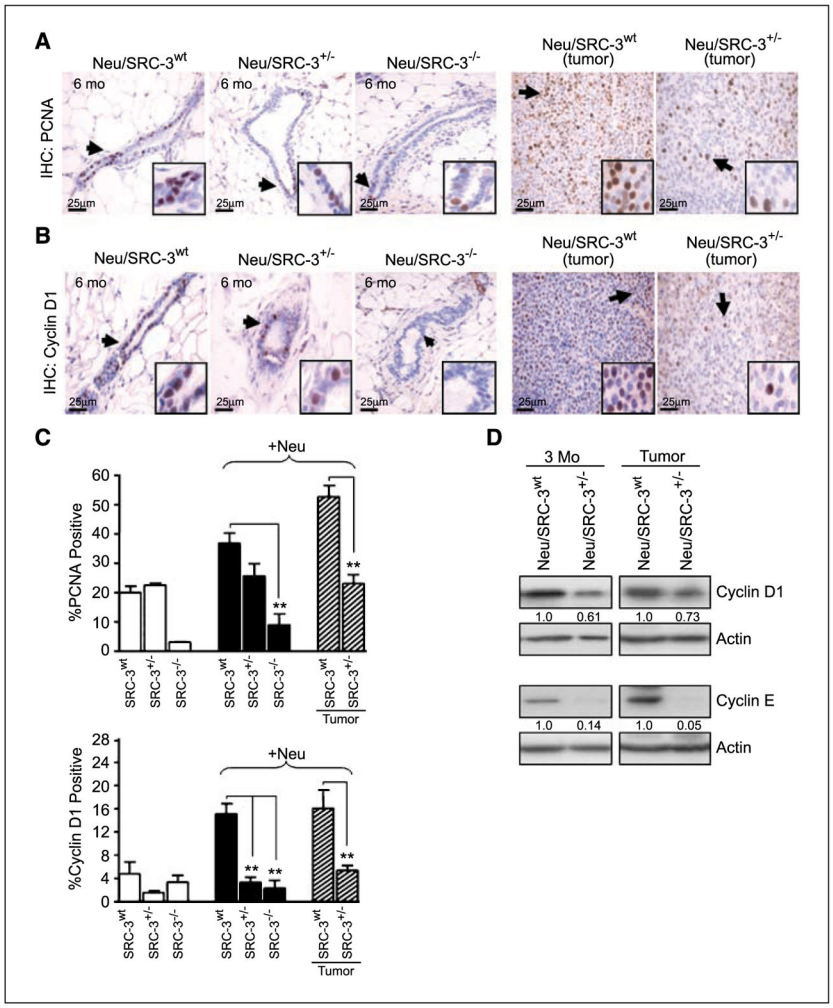

Figure 5.

Lowering SRC-3 levels in MMTV-*Neu* mice reduces epithelial cell proliferation and the expression of cyclins D1 and E. *A* and *B,* representative immunohistochemistries of (*A*) PCNA and (*B*) cyclin D1 expression in mammary gland tissue sections (6 mo of age) and representative mammary tumors from *Neu*/SRC-3^{wt} and *Neu*/SRC-3$^{+/-}$ mice. *Arrows,* positive staining in mammary ductal epithelial cells (magnification, 40×). *C,* bar charts represent the quantification of PCNA and cyclin D1 immunohistochemical staining; 100 cells were counted per field, and 10 fields were counted per mouse (magnification, 40×). *Columns,* mean of three independent experiments; *bars,* SD (n = 3 mice from each indicated genotype). **, $P < 0.001$, one-way ANOVA. *D,* representative Western blot analysis from whole cell extracts prepared from cultured nontumorigenic mammary epithelial cells (3 mo of age) or mammary tumor cells, for cyclin D1 and cyclin E expression. Densitometry values represent cyclin D1 and cyclin E levels normalized to total actin. Western blot results represent data from at least two mice from each genotype.

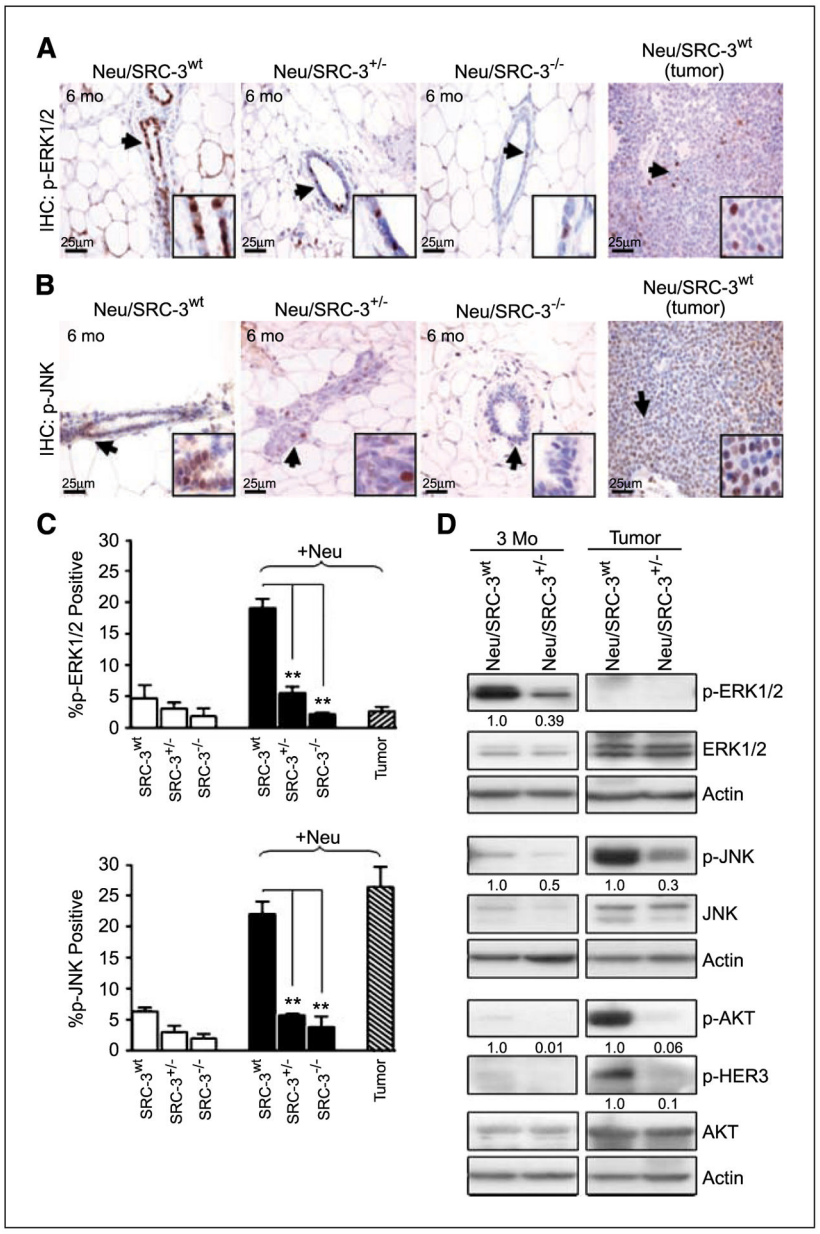

Figure 6.

Lower SRC-3 levels alter *Neu*-mediated signaling in *Neu*-induced mammary gland preneoplasia and tumorigenesis. Representative immunohistochemical staining of p-ERK1/2 (*A*) and p-JNK (*B*) in mammary gland tissue sections (6 mo of age) and representative *Neu*-induced mammary tumor sections. Arrows and insets indicate positive staining in mammary epithelial cells (magnification, 40×). *C,* bar charts represent the quantification of p-ERK1/2 and p-JNK immunohistochemical staining; 100 cells were counted per field, and 10 fields were counted per mouse (magnification, 40×). *Columns,* mean of three independent experiments ($n = 3$ mice from each indicated genotype). **, $P < 0.001$, one-way ANOVA. *D,* representative Western blot analysis of p-ERK1/2, p-JNK, p-AKT, and p-HER3 and their respective total protein expression levels from whole cell extracts of cultured nontumorigenic mammary epithelial cells and tumor cells. Densitometry values represent p-

ERK1/2, p-JNK, p-AKT, and p-HER3 levels normalized to total actin. Western blot results represent data from at least two mice from each genotype.